The paradigm based on the fractal model of granular distribution for the study of the mechanical strength of concrete.

Mhammed Abdeldjalil (mhammed.abdeldjalil@univ-usto.dz)
University of Science and Technology of Oran Mohamed Boudiaf Faculty of Electrical Engineering: Universite des Sciences et de la Technologie d'Oran Mohamed Boudiaf Faculte de Genie Electrique https://orcid.org/0000-0003-1470-4247

Kaddour Chouicha
University of Science and Technology of Oran Mohamed Boudiaf: Universite des Sciences et de la Technologie d'Oran Mohamed Boudiaf

Research Article

Keywords: Granular fractal-identification modulus, Compressive strength, New paradigm, Prediction, Concretes

Posted Date: March 21st, 2022

DOI: https://doi.org/10.21203/rs.3.rs-1415163/v1

Abstract

Studies revealed that all the grain size-grading curves specified by concretes mix designs were all typified by an almost perfect quasi-fractal distribution of the aggregate particle size. This enabled to identify the basic granular mixture (no cement, fine or mineral addition) and determine the porosity, based on the granular fractal-identification modulus"\text{F}\text{D}.\text{l}\text{o}\text{g}(\text{d}/\text{D})", comprising the fractal dimension \left(\text{F}\text{D}\right) of the aggregate involved and the granular range (\text{d}/\text{D}). The aim of this research work was to shed new light on the prediction of concrete mechanical compressive strength - as a major topic addressed by many researchers who investigated concretes - and introduce a new approach to expand the use of the "\text{F}\text{D}.\text{l}\text{o}\text{g}(\text{d}/\text{D})" modulus, which explicitly addressed the aggregate granularity and implicitly determined the related compactness. The approach adopted a two-phase concrete model, where the first phase being the aggregate and the second phase referring to the paste (cement, water, mineral addition and possibly fines). The implemented granular fractal-identification modulus (GFIM) included new parameters of concretes mix designs as dosage and nature of the concrete components, comprising identical aggregates and hence similar (GFIM) and compactness values. Applying a reading array to experimental compiled results of more than 300 concretes selected from literature provided a clear correlation between the development of concrete compressive strength {\text{R}}_{\text{C}28}and a combination of the classical parameters used. The approach thus established a new and more instructive as well as pedagogical paradigm for adequately assessing and controlling concretes performance on fractal basis.

1. Introduction

Mechanical compressive concrete strength is one of the main properties that is strongly required in structural design because either normal or high-performance structural concrete components are basically designed to resist compressive loads. Since the first work of g [1], several studies were carried out to predict the mechanical compressive strength of concretes [2–7]. Therein scientific community, having widely investigated and experimented concrete properties, focused on several parameters and the influence of the component's nature and dosage, in particular. Researchers even sought - through the various concrete formulation methods studied - to establish a state of the art of the related know-how developed so as to provide a solution for the prediction of the concrete mechanical compressive strength. In addition, specialists acknowledged that concretes feature various aggregate properties as chemical and mineral composition, shape, roughness, weathering conditions, specific gravity, hardness, strength, physical and chemical stability, pore structure, mineralogy, surface area, surface texture, particle size and shape, elastic modulus, grading and water absorption, specific surface area, etc. For most studies reported in literature, there is a common ground in that concretes with different mix proportions were expected to be involved and that parameters may be significantly different between approaches, because of the very large number.

As a continuation of works related to fractal analysis, we believed that it is still very appropriate to give the aggregate compactness due importance in addition to parameters including the nature and dosage of the concrete components and contributed to the prediction of the concrete compressive strength. Conversely to the above statements, we applied a reading array to experimental compiled results of more than 300 concretes collected from available literature. We therefore expressed the aggregate compactness employing the implemented granular fractal-identification modulus (GFIM), which is widely detailed herein. To apply the reading array, we used a wide range of experimental works available in the literature and for which the dosage and nature of each concrete components as well as the GFIM were provided. We therefore adopted a two-phase concrete model in that the first phase being the aggregate and the second one referring to the paste (cement, water, mineral addition and possibly fines).

To achieve the intended objective, the following three-staged procedure was adopted. In the former stage of this research work, we comprehensively reviewed what was accomplished in previous research studies regarding some known models for the prediction of the compressive strength of concretes. In this stage, we examined the ability of the reviewed models in predicting the experimental results of the works covered in this research programme. However, since we focused to expand the two-phase model by means of the compactness factor, we explored each method studied looking for direct existence of data on granularity and implicit related compactness. We exceptionally outlined some of the approaches rather briefly because we considered from the very beginning to introduce an alternative approach to investigate concretes considering the parameter (\text{F}\text{D}.\text{l}\text{o}\text{g}(\text{d}/\text{D})that effectively provide granularity for every design mixture. Still in the same stage, application of the fractal distribution to aggregates was then discussed. Noteworthy, one may notice that many authors applied power laws for the so-called reference granular distributions [8]. These laws were identical to the ones used in fractal analysis, especially in the works available in literature. Moreover, those works were also based on the approaches by [9–10], which demonstrated that all concrete mix design methods used aggregates that are distinguished by a quasi-fractal granular distribution (cumulative number of grains as a function of their size). In the next stage and in continuation of the above trend, we addressed all aspects concerning the fractal character of the aggregate size distribution. To do so, we converted all the particle size curves of the experimental data - covering more than 300 mix designs regarding the mechanical compressive strength of concrete - into fractal lines to determine the GFIM (granular fractal-identification modulus). Likewise, we subsequently approached the definition as well as the description of the two-phase model for the multi-parameter concretes studied in [11–13] and expanded the approach by means of the GFIM modulus. The last stage involved the correlation of the results generated by the reading array. This enabled us to draw some conclusions that highlight the didactic and pedagogical potential of this new paradigm in the study of the mechanical compressive strength of concretes. It is clear that this work, it needs another major work to verify the validity of the results obtained, and the reason is that this requires a broad program of work that is very important given the number of parameters to be studied Such as the dosage, the nature of the various components, the coefficient of determination of granular fractals, and other parameters, both conventional and non- conventional.

2. Database Collection And Models Implementation

For the concretes examined, the compressive strengths evaluated using the Féret [1] model show little dispersion and the points are distributed almost along a straight line. Scatters of the compressive strength model of De Larrard [4] are relatively more pronounced but remain small, followed by those of Abrams [2] and Bolomey [3], which exhibit a large dispersion.

This section is based on experimental work in which most of the information referred to must be recorded (Fig. 1). We collected more than 321 types of concrete produced by 20 authors are mentioned in tables (1, 2, 3 and 4) through 59 different research programmes and where different types of concrete mixtures were elaborated. Most countries on the African continent apply European methods, particularly Algeria where French standards are the only ones used. Of the 350 concretes initially collected, 29 were excluded because the sum of the volumes of the components with the volume of air is not equal or does not reach 1000 litres. The compiled experimental results of the selected concretes were collected from different research programmes performed during the period 1992–2018. In most cases, concretes and concretes with added minerals were employed.

In this section, we initiate a comparative survey between experimental results available in the literature and calculated values generated using the above quoted models [1–4]. Figures (2, 3, 4 and 5) illustrates the experimental results of the concretes mechanical compressive strengths ({\text{R}}_{\text{C}28}) versus the values computed using the approaches and models provided by [1–4].

2.1 Description of the enriched biphasic model

2.1.1 Definition of the two-phase model Powers [11], in 1966, takes stock of the evolution of definitions of concrete material. They all retain the biphasic nature with, however, the variations proposed by the various authors. It should be noted that some authors consider the paste to be composed of cement and water (possibly air) while others include the fines which will then be separated from the aggregate.
De Larrard [4] and Yang [12] in his work also uses the two-phase nature of concrete to study the deformation of hardened concrete and the compressive strength. In the paragraph concerning the general model of compressive strength, he specifies that all grains with a diameter greater than 0.08mm will be considered as part of the aggregate and the rest as part of the paste. In the method he developed, he first determines the mechanical strength of the cement matrix before using it to determine the Rc28 of concrete.

Among the many studies using the two-phase model of concrete, that of Benkemoun [15] uses the same model using the finite element method to study the constitution of a new anisotropic model of plasticity. Bonifaz [16] also uses the finite element method with the same model to study concrete.

2.1.2 Enrichment of the two-phase model. We propose to enrich this model by integrating the parameter mentioned in paragraph 3, the GFIM, to account for the influence of the shape of the grain size curve, therefore of the value of DF, on the compactness of the aggregate given the work of [9, 17].
This is not the first time that the role of aggregate compactness has been demonstrated because several authors use this property to propose reference grain size curves [3, 4] showed the influence of the compactness of elementary granular classes on that of the aggregate.

The threshold of 0.1mm remains to be specified depending on the mineralogical nature of the grains, in the literature one will most often find the threshold between 0.08mm and 0.125mm [17].

2.2 Fractal models and granular distribution

All the work of [9–10, 17–19] applied fractal analysis of materials in their respective works. In this study, we apply fractal analysis to aggregates, identifying the granular distribution using the fractal dimension (FD) and the granular range (d/D). The parameter (FD) is calculated by transforming the grain size curves into fractal lines (cumulative number of grains versus their own diameter). Evaluation of the fractal dimension by means of straight fractal lines after transformation of grain size curves is well established in the scientific literature and studies quoted [9–10, 17–19] describe very well the process with detailed information. Moreover, since the fractal line of an ideal fractal object is initially unbounded, we can determine the number of each grain by delimiting this line with parameters (d/D) and assuming all grains are spherical. Several works used the fractal model in civil engineering applications.

2.2.1 Fractal character of high-performance concrete Lecomte and Thomas [19] used fractal analysis to identify granular mixes of high compactness concretes. He pointed out that the minimum porosity may be approximated by a power law, by either [8]' approach or other authors models. This allowed [19] making the link with the fractal approach, using power laws. In fact, [19] studied a distribution of a granular mixtures for a very high-performance concrete and obtained a value of the fractal dimension close to 2.74 (slope of the line equal to -2.74).
2.2.2 Fractal character and granular mix porosity. In the works by [9, 17], it was demonstrated that the parameter (d/D) not only identifies each particle size curve but also the dry granular mixture. This was possible because the approach enabled to determine the design mix porosity-compactness, as shown in the following equation. The approach is therefore based on the assumption that the optimal value of (FD) is 3 (another optimal value can be proposed). The analyses carried out in their respective works yielded a suitable expression "Por(d/D)" (Eq. 1) [9]; for the porosity of a granular mixture, taking into account the porosity of the elementary granular classes "Por(d)" a tightening index (A1) and the curve fitting of the experimental data values using the Gauss-Ampere function.
We introduce in (Fig. 2(a)) a pattern taken from the work of [9]; and in (Fig. 2 (b)) an application to some of works involved in our study. The study by [9]; covered a significant range of the "FD.log (d/D)" factor and whose values were between 0 and − 50. The (FD) value of the design mix studied is noticeably less than 3 and that of "FD.log (d/D)" factor varies from − 4.5 to -7.5. The reason was that only one branch or segment of the initial curve is produced. As shown in (Fig. 2(b)), in this initial curve branch, the (FD) value decreases as the porosity increases at a constant (d/D) value whereas for the other branch both the (FD) value and porosity are decreased:

$$\text{P}\text{o}\text{r}(\text{d}/\text{D})=\text{P}\text{o}\text{r}\left(\text{d}\right)-{\text{A}}_{\text{l}}.{\text{e}}^{\frac{-(\text{F}\text{D}.\text{log}\left(\text{d}/\text{D}\right)-(3.\text{log}\left(\text{d}/\text{D}\right))}^{2}}{2{\text{W}}^{2}}} \quad \text{(Eq. 1)}$$

where Por (d/D) is the Granular mix porosity of (d/D) and $\text{P}\text{o}\text{r}\left(\text{d}\right)$ is the porosity of elementary class (d). "3.log(d/D)" is the optimal fractal granular identification modulus ({\text{F}\text{D}}_{\text{O}\text{p}\text{t}}=3) and "FD.log(d/D) is the fractal granular identification modulus. (W) is the standard deviation as this coefficient describes scattering around optimal value "{\text{F}\text{D}}_{\text{O}\text{p}\text{t}}.\text{L}\text{o}\text{g}(\text{d}/\text{D})" and (A_l) is thetightening coefficient indicating tightening process effect.

In what follows, expression (\text{D}/\text{d}) is rather preferred to (\text{d}/\text{D}) as the minus sign is the sole difference and as expression "{\text{F}\text{D}}_{\text{o}\text{p}\text{t}}-\text{F}\text{D}).\text{log}\left(\text{D}/\text{d}\right)" within the granular mix porosity expression "\text{P}\text{o}\text{r}(\text{d}/\text{D})" is squared and no results change is made.

2.2.3 Fractal character and RVE-model of granular mixtures. In 2012, Sebsadji and Chouicha [10] determined an analytical value of Representative Volume Element (RVE) for a granular mixture (see Eqs. 2 & 3, below), applying fractal analysis of granular mixtures and assuming that each granular mixture is a multiple of an elementary volume:

\text{R}\text{E}\text{V}=\frac{{\text{R}\text{E}\text{V}}_{\text{a}\text{b}\text{s}}}{{\delta }}=\frac{{\text{R}\text{E}\text{V}}_{\text{a}\text{b}\text{s}}}{1-{\text{P}\text{o}\text{r}}_{\left(\text{d}/\text{D}\right)}} (Eq. 2)

{\text{R}\text{E}\text{V}}_{\text{a}\text{b}\text{s}}=\sum _{\text{i}=1}^{\text{n}}{\text{N}}_{\text{\varnothing }\text{i}}{\text{V}}_{\text{\varnothing }\text{i}} (Eq. 3)

where (REV) is the Representative Elementary Volume and (REV_{abs}) is the representative elementary absolute volume. (δ) is the volume content of granular mix compactness and "{\text{P}\text{o}\text{r}}_{(\text{d}/\text{D})}" is the granular mix porosity for a (d/D) granular extent, corresponding to that of a fresh concrete. ($N_{\phi i}$) is the representative elemental number of grains with dimension (φ_i) and ($V_{\phi i}$) is the elementary volume of a grain with dimension (φ_i).

3. Concretes Mechanical Compressive Strength Models

In this section, we introduced some of the existing models for the prediction of the compressive strength of concrete, which we applied in order to verify their ability to predict the experimental values of existing concrete mix designs. In this context, we wish to mention the works of Féret (1892) as represented in Eq. (4), Abrams (1918) proposed a rather simple exponential equation of the type shown in the following Eq. (5), Bolomey (1936) approach Eq. (6) focuses on the main role played by cement (mass and real class) and water, More recently, De Larrard (2000) provided a more elaborate model for the evaluation of the compressive strength of the material. The following model relationship see equations (7, 8) below is intended to predict the compressive strength of cured Portland cement-based concretes, at 28 days. Also, since we focused on contributing to the improvement of the two-phase model by using the compactness factor, we thoroughly explored the occurrence of granularity and thus implicitly compactness data for each method examined. We therefore only briefly highlighted some of these approaches as we proposed an alternative procedure to study concrete, enabling the parameter FD.log (d/D) to provide full value for the mix design granularity. Only then, we proceeded to consider the application of fractal distribution to aggregates.

- Féret's formula – 1892

\text{R}=\text{k}{\left(\frac{\text{C}}{\text{C}+\text{W}+\text{V}}\right)}^{2}
4
where (R) is the concrete mechanical compressive strength, (k) the coefficient depending on cement class aggregates type and preparation method, (C) the cement content, (W) the water content and (V) the subsisting volume of air.

- Abrams formula – 1919

{\text{f}}_{\text{c}}=\text{a}\text{*}{\text{b}}^{\text{W}/\text{C}}
5
where ({\text{f}}_{\text{c}}) is the mechanical strength of concrete, (a) and (b) are two controlling constants on which the exponential expression depended and (w/c) is the cement-to-water ratio.

The basic values of the two constants (a) and (b) are approximately 147 and 0,0779, respectively. Once again, only water and cement contents are taken into account in this equation. The implementation of this approach involves the selection of the slump, the D-value, the estimation of the quantity of gravel with measurement of its density by tapping and the use of the modulus of fineness of the sand as well as the calculation of the mass of sand involved. The aggregate considered is divided into two families (gravel and sand), thus little is actually understood about granularity.

- Bolomey formula – 1936

{\text{R}}_{\text{c}28}=\text{G}.{{\sigma }}_{\text{c}28}^{{\prime }}\left(\frac{\text{C}}{\text{W}}-0.5\right)
6
Here, ({\text{R}}_{\text{c}28}) is the concrete mechanical compressive strength at 28 days. \left(\text{G}\right) is the coefficient that is related to the aggregate type, between 0.35 and 0.65, ({{\sigma }}_{\text{c}28}^{{\prime }}) is the real cement class or real mechanical strength of standardised cement-mortar and (\text{c}/\text{w}) is the cement-to-water ratio.

- De Larrard formula – 2000

{\text{f}}_{\text{c}}={\text{K}}_{\text{g}}{\text{R}}_{\text{C}\text{V}}{\left(\frac{{\text{V}}_{\text{c}}}{{\text{V}}_{\text{c}}+{\text{V}}_{\text{w}}+{\text{V}}_{\text{a}}}\right)}^{2}{\text{M}\text{P}\text{T}}^{-\text{0,13}}
7
In this relation, ({\text{f}}_{\text{c}}) is the compressive strength of concrete and ({\text{K}}_{\text{g}}) is the coefficient describing the effect of the aggregate over the compressive strength. ({\text{R}}_{\text{c}\text{v}}) is the mechanical strength of cement real class, ({\text{V}}_{\text{a}}) is the volume of air included

in unit volume of cement fresh paste, ({\text{V}}_{\text{c}}) is the volume of cement in unit volume of cement fresh paste and {(\text{V}}_{\text{w}}) is the volume of water in unit volume of cement fresh paste. Finally, \left(\text{M}\text{P}\text{T}\right) is the maximum paste thickness expressed as:

\text{M}\text{P}\text{T}={\text{D}}_{\text{m}\text{a}\text{x}}(\sqrt[3]{{\text{g}}^{\text{*}}/\text{g}}-1)
8
where \left({\text{D}}_{\text{m}\text{a}\text{x}}\right) corresponds to the 90% mixture passing aggregate and\left(\text{g}\right) is the granular volume within a unit volume of concrete and both parameters are easily defined from the mixture formulation; (g*) defines the real compactness of the same aggregate, which may either be measured or evaluated by means of the MEC model of De Larrard (2000) and Boukli et al. (2014).

For the concretes examined, the compressive strengths evaluated using the Feret [1] model show little dispersion and the points are distributed almost along a straight-line, Fig. 3. Scatters of the compressive strength model of De Larrard [4] are relatively more pronounced but remain small Fig. 4, followed by those of Abrams and Bolomey [2, 3] Figs. 5 and 6, which exhibit a large dispersion.

4. Implementation Of The Fractal Model

Studies by [9] and [10] showed that concretes with different mix designs exhibit an almost perfect fractal distribution for the grain size of concrete aggregates. This observation is again validated in this work where different concretes manufactured from 1992 to 2018 were studied. Figure 7 is an illustrative example that demonstrates the transformation of granular distributions into fractal distributions for Dhir [20]. The granular mixtures are clearly identified using the fractal dimension (FD) and the granular range (d/D).

The particle size curves of all the basic granular mixtures used display a value of the fractal dimension ({\text{F}\text{D}}_{\text{g}}) between 2.30 and 3.00 while all the particle size curves of all the granular mixtures with cement, fine mineral and addition feature a value of the fractal dimension ({\text{F}\text{D}}_{\text{c}}) ranging between 2.55 and 2.85. In accordance with the two-phase concrete model, the base aggregate comprises no additives or fines. In all cases, the value of the correlation coefficient proves that it is a quasi-fractal distribution.

By considering the fractal dimension (\text{F}\text{D}) of the granular mixtures and their granular extent (d/D), we can express (Eq. 9) for a basic granular mixture without cement and mineral additions, and (Eq. 10) for a granular mixture with cement and active additions. The maximum size (\text{D}) of the aggregate for both mixtures is the same. However, there are two minimum dimensions, namely the first is for ({\text{d}}_{\text{g}}) basic granular mix and the second is smaller than the first for ({\text{d}}_{\text{c}}) granular concrete mix.

{\text{G}\text{F}\text{l}\text{M}}_{\text{g}}={\text{F}\text{D}}_{\text{g}}.\text{l}\text{o}\text{g}(\text{D}/{\text{d}}_{\text{g}}) (Eq. 9)

{\text{G}\text{F}\text{l}\text{M}}_{\text{c}}={\text{F}\text{D}}_{\text{c}}.\text{l}\text{o}\text{g}(\text{D}/{\text{d}}_{\text{c}}) (Eq. 10)

In which ({\text{G}\text{F}\text{l}\text{M}}_{\text{g}}), ({\text{G}\text{F}\text{l}\text{M}}_{\text{c}}), ({\text{F}\text{D}}_{\text{g}}) and ({\text{F}\text{D}}_{\text{c}}) are, respectively, the fractal granular identification modulus of basic granular mixtures and of concrete and the fractal dimensions of basic granular mixtures and of concrete. Finally, (\text{D}), ({\text{d}}_{\text{g}}), ({\text{d}}_{\text{c}}) are, respectively, the maximum grains size the minimum grains sizes of basic granular mixtures and of concrete. Tables 1 to 4 provide the variation in the values of the fractal dimension of the basic granular mixture as well as that of the fractal modulus of granular identification for all the works of the authors from the four continents.

The Table 3 and Table 4, in supplementary materials (Supporting Information) contains the results of the concretes studied by the [26], whose work cited us, which used aggregates from a few American quarries, and [37–39] which used the aggregates from some quarries of Asia.

The Table n ° 1 above contains the identification results of the granular mixtures of bases used in the concretes studied by the authors [19–25] of which their work cited to us during the data collections, noting that the aggregates used come from some European quarries.

Table 1
Concrete having the same {\text{G}\text{F}\text{l}\text{M}}_{\text{g}} and {\text{F}\text{D}}_{\text{g}} values of some works by European

Authors, Year & Ref.	Total number T_N		Modulus{\text{G}\text{F}\text{l}\text{M}}_{\text{g}}	Fractal Dimension	
	Concretes	{\text{G}\text{F}\text{l}\text{M}}_{\text{g}}		{\text{F}\text{D}}_{\text{g}}	R^2
Lecomte (1992)	3	0			
De Larrard [2001)	5	0			
Zennir (1996)	9	9	6.59	2.64	0,9
Dhir (2005) - PC	12	2	6.27	2.51	0,9
		2	6.12	2.45	0,9
Dhir (2005) - PFA	15	2	6.52	2.61	0,9
		2	6.45	2.58	0,9
Dhir (2005) - Mixt	11	2	6.20	2.48	0,9
		2	6.32	2.53	0,9
		3	6.42	2.57	0,9
		3	6.45	2.58	0,9
Meddah (2010)	4	0			
Hager, Gawęska [2015	1	0			
Roziere (2009)	1	0			

The Table 2 also contains the results of the concretes studied by the authors [27–36] whose work cited us, which used the aggregates coming from quarries in some countries located in the north of the African continent.

Table 2
Concrete having the same {\text{G}\text{F}\text{l}\text{M}}_{\text{g}} and {\text{F}\text{D}}_{\text{g}} \text{v}\text{a}\text{l}\text{u}\text{e}\text{s}of some v

Authors, Year & Ref.	Total number TN		Modulus{\text{G}\text{F}\text{l}\text{M}}_{\text{g}}	Fractal Dimension
	Concretes	{\text{G}\text{F}\text{l}\text{M}}_{\text{g}}		{\text{F}\text{D}}_{\text{g}}
Mehamdia (2015)	6	6	6.91	2.77
Guemmadi (2009)	26	23	6.39	2.56
Joudi (2012)	15	3	6.71	2.69
		3	6.76	2.71
		6	6.79	2.72
		3	6.84	2.74
Achour (2008)	18	0		
Rabehi (2014)	8	2	6.26	2.72
		2	6.21	2.70
		2	6.14	2.67
Boukli (2009) DA	17	17	6.90	2.66
Boukli (2009) DM	17	17	6.93	2.67
Saadani (2000)	15	2	6.41	2.57
		2	6.44	2.58
		2	6.49	2.60
		2	6.56	2.63
Benouis (2011)	7	2	6.83	2.63
Mennaai (2008)	1	1	5,99	2,50

T_N: Total number of concretes. {\text{G}\text{F}\text{l}\text{M}}_{\text{g}} : Total number of concretes with the same {\text{G}\text{F}\text{l}\text{M}}_{\text{g}}

5. Relevant Parameters For Rc28

5.1 Effect of conventional parameters

Of all the parameters mentioned in the introduction and that have a direct influence on the concrete mechanical strength, only some conventional ones such as (\text{c}/\text{w}) together with ({\text{K}}_{\text{c}}), ({\text{d}}_{\text{m}\text{g}}), (Kg), ({\text{M}}_{\text{f}}), ({\text{M}}_{\text{A}\text{d}\text{m}}) and ({\text{K}}_{\text{A}\text{d}\text{m}}), (\text{G}/\text{S}) as well as some less conventional ones like (\text{D}/{\text{d}}_{\text{g}}), (\text{D}/{\text{d}}_{\text{c}}), ({\text{F}\text{D}}_{\text{g}}), ({\text{F}\text{D}}_{\text{c}}), "\text{P}\text{o}\text{r}(\text{D}/\text{d})" were used in the following sub-sections. This selection campaign allowed specifying parameters, which may primarily be integrated in the analysis in order to achieve the planned objectives.

It is clear that of all the parameters, only a small number are included in the analysis because not only are some difficult to identify and/or quantify but also, they hardly affect the mechanical strength of the concrete in any significant extent compared to the classical parameters. To [18], for instance, the actual shape of the aggregates is a case where fractal analysis seems to provide a solution.

5.1.1 C/W effect - as conventional parameter - to all authors' works. Figure 8 shows that some concretes [26, 34, 38] exhibit different values of the mechanical compressive strength whereas (c/w) ratio remains constant. Use of different contents and classes of cement between authors generates a large dispersion. Thus, taking into account only the (c/w) ratio as a decisive factor is totally irrelevant and inappropriate. Conversely to [22, 33] values of some other concretes mechanical compressive strengths seem well distributed on either side of a straight line for a varying (c/w) ratio (see also Fig. 8). These three latter works are very particular because authors used concretes with identical basic granular mix, i.e. concretes providing a similar ({\text{G}\text{F}\text{l}\text{M}}_{\text{g}}) value (Eq. 9), as indicated in Tables 1 to 4.

5.1.2 C/W effect - as conventional parameter - to each author's work. We provide here a study, by author, which illustrates the effect of (c/w) on the compressive strength of concrete, Figs. 9, 10 and 11. Since we intend to study the influence of the ratio in the works of each author, we do not need to use the actual or standardised class of cement, unless some authors use different classes in the same work.

Graphs in Fig. 9 (a, b, c, d) indicate that when the correlation factor is high, this implies that the same basic granular mix is used for the concretes produced by each author. This is evidenced by little or no change in (\text{G}/\text{S}) as well as no change in parameters such as ({\text{F}\text{D}}_{\text{g}}), ({\text{d}}_{\text{g}}), ({\text{d}}_{\text{c}}) and (\text{D}) and a change in ({\text{F}\text{D}}_{\text{c}}). However, (c/w) ratio varies significantly, sometimes showing double and intermediate ratios. Hence, the explanation for the variation of the compressive strength of concrete with (c/w) ratio and the increase of the correlation factor. This type of concrete proves the relevant contribution of (c/\text{w}) ratio in assessing concrete mechanical compressive strength for an almost similar basic granular mixture.

For the subsequent three authors' concretes presented in Figs. 10 (a, b, c, d) and for which the correlation is either weak as for [29] and [30] or remains significant as in the case of [20] the evaluation of the different ingredients allowed to evaluate the variation of the (c/w) ratio as well as the granular content. This is again evidenced by the considerable variability of (\text{G}/\text{C}) or of both ({\text{F}\text{D}}_{\text{g}}) and of ({\text{F}\text{D}}_{\text{c}}). In addition, this suggests once again that the parameters related to the binder, the paste and the grains size curves are also relevant parameters and need all be taken into account must all be taken into account. Further, variation of the (c/w) ratio alone is still not sufficient to account for the evolution of any concrete ({\text{R}}_{\text{c}28})mechanical compressive strength.

Considering the last graphs of Fig. 11 (a, b, c, d) with zero correlation, the (c/w) ratio of the examined concretes either varies or may even remain constant while the basic granular mixture shows considerable variations. This is clearly evidenced for such concretes by the variation of both ({\text{F}\text{D}}_{\text{g}}) and ({\text{F}\text{D}}_{\text{c}}) factors whereas the (\text{G}/\text{S}) ratio varies or being approximately constant. As previously stated by [9], this further validates that ({\text{F}\text{D}}_{\text{g}}) and ({\text{F}\text{D}}_{\text{c}}) may also be considered as relevant parameters as they tell more than (G/S) about the granularity. Finally, (\text{c}/\text{w}) ratio is nor relevant nor inappropriate alone for the concrete ({\text{R}}_{\text{C}28})mechanical compressive strength evolution. Tables (1, 2) and Tables (3, 4 in Supplementary Materials) provides the whole range of concretes carried out by different authors, considering concretes with various and similar values of "{\text{F}\text{D}}_{\text{g}}.\text{l}\text{o}\text{g}\left({\text{D}/\text{d}}_{\text{g}}\right)" parameter.

5.1.3 Effect of conventional parameters \mathbf{G}/\mathbf{S} **and** {\mathbf{d}}_{\mathbf{m}\mathbf{g}} To account for the mechanical strength of aggregates, we adopted the classifications of [3] and [21], which allocate a coefficient value ({\text{K}}_{\text{g}}) to each aggregate type. The two known parameters ({\text{d}}_{\text{m}\text{g}}) and ({\text{K}}_{\text{g}}) are not relevant when taken separately since for the same values of the two known parameters v the value of ({\text{R}}_{\text{c}28}) changes. For [28, 29, 33], on the other hand, ({\text{R}}_{\text{c}28}) varies with a constant (\text{G}/\text{S}) ratio and there are cases in which the ({\text{R}}_{\text{c}28}) varies with the (\text{G}/\text{S}) ratio without being able to identify a common correlation. In the work of [21], ({\text{R}}_{\text{c}28}) decreases with the increase of (\text{G}/\text{S}) while it increases regularly with the increase of (\text{G}/\text{S}) in the work of [19]. Those results enhance the fact that (\text{G}/\text{S}) ratio alone may not be regarded as a relevant parameter to fully understand the mechanical behaviour of the concretes.

5.2 Effect of non-conventional parameters

This section is devoted to assess the relevance of some non-conventional parameters, aimed at the determination of their influence on concretes mechanical compressive strength ({\text{R}}_{\text{C}28}). We particularly focus our attention on the porosity of granular mix designs without cement, fines and mineral additions, using the mathematical expression derived by [9]; (see related sub-sections). We will then use the parameters "{\text{F}\text{D}}_{\text{g}}.\text{l}\text{o}\text{g} \left({\text{D}/\text{d}}_{\text{g}}\right)" and "{\text{F}\text{D}}_{\text{c}}.\text{l}\text{o}\text{g} \left({\text{D}/\text{d}}_{\text{c}}\right)".

5.2.1 Porosity of granular mixes - Por (D/d) It can be seen in Fig. 12 that for the same values of the cement free granular mixture porosity, whether by author or between authors, the value of ({\text{R}}_{\text{C}28}) differs, hence the need to integrate other parameters. For instance, concretes of [27] are different in their porosity values Fig. 10.

5.2.2 Granular fractal-identification modulus {\mathbf{G}\mathbf{F}\mathbf{l}\mathbf{M}}_{\mathbf{g}} **and** {\mathbf{G}\mathbf{F}\mathbf{l}\mathbf{M}}_{\mathbf{c}}We may notice from Fig. 13 that concretes can have the same value of the modulus ({\text{G}\text{F}\text{l}\text{M}}_{\text{g}}) - see (Eq. 9) - but different values of ({\text{F}\text{D}}_{\text{g}}) for concretes of [28] and those of [33]. This is why we are to identify each basic granular mixture by ({\text{G}\text{F}\text{l}\text{M}}_{\text{g}}) and ({\text{F}\text{D}}_{\text{g}}). One may also notice that for the same parameter values of ({\text{G}\text{F}\text{l}\text{M}}_{\text{g}}) or ({\text{F}\text{D}}_{\text{g}}) alone, whether by author or between authors, there is variation in the value of ({\text{R}}_{\text{C}28}) value, hence the need to consider other parameters.

Comparison of the depicted experimental results shows that - even for works by [28, 22, 29], concretes endowed with identical values of ({\text{F}\text{D}}_{\text{c}}) and ({\text{G}\text{F}\text{l}\text{M}}_{\text{c}}) - see (Eq. 10) - show small variations when parameters ({\text{F}\text{D}}_{\text{c}}) and ({\text{G}\text{F}\text{l}\text{M}}_{\text{c}}) are used. Therefore, even basic granular mixes may engender differences in concretes when some components such as cement, fines, mineral additions and - of course water - are included. However, the variations are not considerably larger as there is not considerable variability in ({\text{G}\text{F}\text{l}\text{M}}_{\text{c}}) values with those concretes. Conversely, this phenomenon does not occur with concrete in the works of [21, 37,33) for which there is constriction of ({\text{G}\text{F}\text{l}\text{M}}_{\text{c}}) values with respect to the related range of ({\text{G}\text{F}\text{l}\text{M}}_{\text{g}}) values and whose basic granular mixes were different but provided nearly similar concretes. In accordance with Table 1, we may also notice - for instance - that in the case of Achour's concretes [27], the values of ({\text{F}\text{D}}_{\text{c}}) and ({\text{G}\text{F}\text{l}\text{M}}_{\text{c}}) are widely scattered, hence the difficulty of using this work. The same difficulty is experienced when using Saadani's concretes [34]. Indeed, although there is a tightening of the concretes as evidenced by the small variation in ({\text{G}\text{F}\text{l}\text{M}}_{\text{c}}), the basic granular mixtures are still different.

In his work, [9]; insisted on the relevance of (GFIM) factor to determine the porosity value of basic dry granular mixes. Also, the above results discussed earlier in sub-section show that there is an evident correlation between concretes mechanical compressive strength ({\text{R}}_{\text{C}28}) and (\text{c}/\text{w})ratio for concretes with the same ({\text{G}\text{F}\text{l}\text{M}}_{\text{g}}) value. Given these two results, we decided to emphasise that concretes prepared with similar base granular mixtures and with identical ({\text{G}\text{F}\text{l}\text{M}}_{\text{g}}). For this purpose, we initially use the works where all concretes of the same author are prepared with the same basic granular mixture [22, 31], i.e. concretes with the same ({\text{F}\text{D}}_{\text{g}}), (\text{D}) and ({\text{d}}_{\text{g}}) values. We then select some concretes with identical "{\text{F}\text{D}}_{\text{g}}.\text{l}\text{o}\text{g}(\text{D}/{\text{d}}_{\text{g}}" values and, in particular, those incorporating fines [29]. We may eventually consider more works in which two and/or three concretes types that have the same value of ({\text{G}\text{F}\text{l}\text{M}}_{\text{g}}) are used. However, we cannot come up with useful information since two points will always produce a straight line while three points are insufficient to detect the behaviour trend.

5.2.3 Granular fractal-identification modulus {\mathbf{G}\mathbf{F}\mathbf{l}\mathbf{M}}_{\mathbf{g}} **and** {\mathbf{S}}_{\mathbf{s}} The influence of conventional parameters such as (\text{C}/\text{W}) together with ({\text{K}}_{\text{c}}), ({\text{M}}_{\text{f}}), ({\text{M}}_{\text{A}\text{d}\text{m}}) with ({\text{K}}_{\text{A}\text{d}\text{m}}) and (\text{G}/\text{S}) was extensively investigated. In this case, we study the effect of the cement class with respect to ({\text{K}}_{\text{c}}) parameter:

{\text{K}}_{\text{c}}= (52.5/{\text{R}}_{\text{s}\text{c}}) (Eq. 11)

In (Eq. 11), the relation of ({\text{K}}_{\text{c}}) to ({\text{R}}_{\text{s}\text{c}}) of a normalised cement class is determined using the standardised cement class to the potentially maximum class ratio, being equal to 52.5 MPa. However, we considered cement standardised class because of the lack of adequate quality data on the true class of cement within some authors' works. The influence of the types of mineral additions is taken into account through the use of ({\text{K}}_{\text{A}\text{d}\text{m}}) in accordance with NF EN 206 + A1 [40].

To [21], who already addressed the influence of the specific surface of fillers, this latter has two effects, namely an accelerating role and a binding effect depending on the aluminates blended in the cement. [38] pointed out the importance of the specific surface of cements. The type of fines is analysed using the specific surface developed and calculated as the sum of the surface of all the grains divided by the total mass of the fines concerned, in (m^2/kg). In the work of [29], the value of the Blaine specific surface is well established. However, this value is replaced with that determined by previous calculations in order to provide a homogeneous representation for all the fines used by the other different authors.

As previously explained, the experimental study presented in [29] work enabled to fully appreciate the influence of fines. In details and as illustrated in Fig. 10, the initial experimental curve showing the evolution of ({\text{R}}_{\text{C}28}) as a function of the (\text{c}/\text{w}) ratio exhibited a very poor correlation. In order to be representative, we therefore decided to select only concretes endowed with the same value of the granular fractal-identification modulus ({\text{G}\text{F}\text{l}\text{M}}_{\text{g}}) of basic granular mixes shown in Fig. 13(a, b, c, d). Again, this latter figure illustrates the evolution of ({\text{R}}_{\text{C}28}) as a function of (c/\text{w}) and provides the same features as that mentioned above. On the other hand, we added the used ({\text{S}}_{\text{S}}) fines value to ({\text{G}\text{F}\text{l}\text{M}}_{\text{g}}). Using these two relevant indicators, Fig. 13(b) demonstrates, on the basis of the results obtained, that the investigated concretes provide a better understanding of the role of the fines with respect to all their ({\text{S}}_{\text{S}}) values.

It is worth noting that reading of Fig. 13(b) curve becomes profitably easy. In addition, it expresses a result found by the author who specifies that for fines (F5), the Blaine and calculated specific surface are 540m^2/kg and 729.7 m^2/kg, respectively and that for fines (F10) the respective values are equal to 450 m^2/kg and 441.2 m^2/kg. In addition, there is an optimum value (18%) for the fines dosage. However, for fines (F29) whose respective Blaine and calculated specific surface are 265m^2/kg and 206.5 m^2/kg, the experiment may not reach this optimum dosing value. It is also worth noting that when this optimum dosage is exceeded, ({\text{R}}_{\text{C}28}) decreases due to the increase of the volume of solid grains and liquid ratio, which reduces workability and hence compactness in terms of the installation used. Hence the decrease in ({\text{R}}_{\text{C}28}).

Partial outcomes achieved in the works of [32] work are illustrated in Figs. 13 (c, d), respectively. These demonstrate that changing the specific surface area of the cement (different grain size curves) lead to different curves with constant values of (c/w) ratio. This is why we decided to integrate as a relevant parameter comprising the specific surface of the cement and mineral additions and calculated using the same method as for fines.

The above analysis permitted to first conclude that it is necessary to consider cement (C) with ({\text{K}}_{\text{C}}) as well as ({\text{M}\text{i}}_{\text{A}\text{d}\text{m}}) mineral additions with ({\text{K}\text{i}}_{\text{A}\text{d}\text{m}}) and ({\text{M}}_{\text{f}}) fines with their respective values of ({\text{S}}_{\text{S}\text{f}}) and ({\text{S}\text{i}}_{\text{S}\text{A}\text{d}\text{m}}). The (i) symbol is introduced because in some works more than one mineral addition is used.

On the other hand, and knowing that dosage and type of the mix designs vary, it is no longer appropriate to carry out a survey with only C/W but to effectively take into account the expression of the ratio of the paste components of the (\text{B}) binder and of the (w) water:

\text{B}=\left(\left(\text{C}\times {\text{K}}_{\text{C}}\times {\text{S}}_{\text{S}\text{c}}\right)+({\text{M}}_{\text{f}}\times {\text{S}}_{\text{S}\text{f}})+(\sum _{\text{i}}{\text{M}\text{i}}_{\text{A}\text{d}\text{m}}\times {\text{K}\text{i}}_{\text{A}\text{d}\text{m}}\times {\text{S}\text{i}}_{\text{S}\text{A}\text{d}\text{m}})\right)/(1000\times \text{W}) (Eq. 12)

- Fines of active mineral additions.

\sum _{\text{i}}{\text{M}\text{i}}_{\text{A}\text{d}\text{m}}\times {\text{K}\text{i}}_{\text{A}\text{d}\text{m}}\times {\text{S}\text{i}}_{\text{S}\text{A}\text{d}\text{m}})

- Fines of inert fillers.

{(\text{M}}_{\text{f}}\times {\text{S}}_{\text{S}\text{f}})

- Fines of cementitious binders.

\left(\text{C}\times {\text{K}}_{\text{C}}\times {\text{S}}_{\text{S}\text{c}}\right)
As we had to work with the same basic granular mixtures therefore finally the ({\text{R}}_{\text{C}28}) will be studied according to:

{{\text{G}\text{F}\text{l}\text{M}}_{\text{g}}}^{\left(\text{B}\right)/(1000\times \text{W})} (Eq. 13)

The above conclusions are emphasised by the explanations given above (the above in sub-section) where it was already decided to determine ({\text{F}\text{D}}_{\text{g}}) and ({\text{G}\text{F}\text{l}\text{M}}_{\text{g}}) excluding fines and mineral additions but to evaluate ({\text{F}\text{D}}_{\text{c}}) together with ({\text{G}\text{F}\text{l}\text{M}}_{\text{c}}) incorporating both components. For, we divide the value of (\text{C}.{\text{R}}_{\text{s}\text{c}}) by 52.5 MPa (maximum standardised strength) and by 1000 m^2/kg (maximum specific surface ({\text{S}}_{\text{S} }) for cement, fines and mineral additions) so as not to carry a large value and make measurement units homogeneous.

6. Analyses And Discussion

In what follows, we will apply the results we achieved, i.e. the use of the parameter appearing in the following Eqs. (14) and (15):

B/W=\left(\left(\text{C}\times {\text{K}}_{\text{C}}\times {\text{S}}_{\text{S}\text{c}}\right)+{(\text{M}}_{\text{f}}\times {\text{S}}_{\text{S}\text{f}}))+(\sum _{\text{i}}{\text{M}\text{i}}_{\text{A}\text{d}\text{m}}\times {\text{K}\text{i}}_{\text{A}\text{d}\text{m}}\times {\text{S}\text{i}}_{\text{S}\text{A}\text{d}\text{m}}))\right)/\text{W} (Eq. 14)

Converting the ratio unit (B/W) from (kg/l) to (kg/m^3), so writes the expression (B/W.1000). After (Eq. 14), we have:

{\text{R}}_{\text{C}28\cong }{{\text{G}\text{F}\text{l}\text{M}}_{\text{g}}}^{\left(\text{B}/1000.\text{W}\right)} (Eq. 15)

where (R_{C28}) is the compressive strength of concrete at 28 days, ({\text{G}\text{F}\text{l}\text{M}}_{\text{g}}) is the granular fractal-identification modulus of basic granular mix. (\text{B}/\text{W}) is the ratio of equivalent cement-to-water, (\text{C}), ({\text{K}}_{\text{c}}) and ({\text{S}}_{\text{s}\text{c}}) is respectively the cement content, the factor of standard class and the specific surface, respectively. ({\text{M}}_{\text{f}}) and ({\text{S}}_{\text{s}\text{f}}) are, respectively, the aggregate fine particles content and the related specific surface. Finally, ({\text{M}}_{\text{A}\text{d}\text{m}}) and ({\text{K}}_{\text{A}\text{d}\text{m}}) and ({\text{S}}_{\text{s}\text{A}\text{d}\text{m}}) are, respectively, the mineral additions content, the factor of equivalent and the specific surface.

Graphs of the selected concretes are shown in Figs. 14 and 15 below. The curves are obtained by applying formula (15) for the works already planned in the above in sub-section. To achieve such objectives, we investigated identical basic granular mixes having the same ({\text{F}\text{D}}_{\text{g}}) and ({\text{G}\text{F}\text{l}\text{M}}_{\text{g}}) values to end up with concretes defined by ({\text{F}\text{D}}_{\text{c}}) and ({\text{G}\text{F}\text{l}\text{M}}_{\text{c}}) values, as well as the specific surface area ({\text{S}}_{\text{S}}).

6.1 Concrete of the same basic granular mix.

Figure 14(a), Illustrates the results of the analysis of the concrete compressive strength, according to the new model. We have presented the concretes of [22, 28, 29, 31] which used the same granular mixtures of bases for several concretes.

Figures 14 (a), (b), (c), (d), seems to indicate the evolution of the (R_{C28}) of a concrete with the dispersions inherent in the tests [28, 29], but taking ($GFIM_g$) and, ($GFIM_c$) and fines (S_{Sf}) into account shows that these are test results on the different concretes in Fig. 13(a, b).

Figures 14 (e), (f), seems to indicate the evolution ({\text{R}}_{\text{C}28}) of the concretes [22, 31] taking into account ({\text{G}\text{F}\text{l}\text{M}}_{\text{g}}) which shows that these are results of the concretes included of the basic granular mixtures of the same value ({\text{G}\text{F}\text{l}\text{M}}_{\text{g}})

6.2 Adjustment of the experimental curves

The present work focused on the evolution of the value of ({\text{R}}_{\text{C}28}). We therefore assumed a fit using two forms for all the experimental curves obtained for the types of concretes explored. Also, we proposed first the Gauss Ampère function:

\text{Y}={\text{Y}}_{0}+\text{A}\times {\text{e}}^{{-(0.5\times (\text{X}-{\text{X}}_{\text{o}\text{p}\text{t}\text{i}\text{m}\text{a}\text{l}}))}^{2}/{{\omega }}^{2}} (Eq. 16)

and in the case of acceptable correlation or otherwise, the following simplified exponential function is used:

\text{Y}={\text{Y}}_{0}+\text{A}\times {\text{e}}^{(\text{R}\times \text{X})} (Eq. 17)

The curves of Fig. 15 are obtained by applying formulas (15), (16), (17) for the work already planned according to the identical concretes having the same values ({\text{F}\text{D}}_{\text{g}}) and ({\text{G}\text{F}\text{l}\text{M}}_{\text{g}}) and the values ({\text{F}\text{D}}_{\text{c}}) and ({\text{G}\text{F}\text{l}\text{M}}_{\text{c}}), as well as the specific surface ({\text{S}}_{\text{S}}).

Figure 5(a) and (b) are shown the concrete results for [28], according to an extrapolation analysis by the Gauss-Amper function and the Exponential, according to different values of {\text{G}\text{F}\text{l}\text{M}}_{\text{C}}.

Figures 15(c) and (d) are shown the concrete results an extrapolation analysis by the Gauss-Ampere for [29] according to different values of{ \text{S}}_{\text{S}\text{f}}, and for [20] Shapes of curves obtained using fitting in terms of number of points (concretes).

Figures 15 (e) and (f) for extrapolation analysis of the Gauss-Ampere and Exponential for [22] according to different values of {\text{G}\text{F}\text{l}\text{M}}_{\text{g}}., and for [31] the Gauss-Ampere according to different values of {\text{G}\text{F}\text{l}\text{M}}_{\text{g}}.

6.3 About the prediction of{\mathbf{R}}_{\mathbf{C}28}

Another stand-alone work that follows this complete work to validate the theoretically expected results. Therefore, as a possible expedient trend for gaining confidence with the proposed approaches, further experimental investigations are needed on a large range of concretes for which the ({\text{G}\text{F}\text{l}\text{M}}_{\text{g}}) and ({\text{F}\text{D}}_{\text{g}}), ({\text{S}}_{\text{S}}) Table 5, value is the same as that for which fittings were made.

Table 5
Concrete has the same {\mathbf{G}\mathbf{F}\mathbf{l}\mathbf{M}}_{\mathbf{g}} values, and different for {\mathbf{G}\mathbf{F}

Authors & ref	Fit Formula	TN of C	{\mathbf{G}\mathbf{F}\mathbf{l}\mathbf{M}}_{\mathbf{g}}	{\mathbf{G}\mathbf{F}\mathbf{l}\mathbf{M}}_{\mathbf{
Zennir [22]	Extrapolation Exponential	03	6,59	13,14
		03		13,33
		03		13,52
Boukli [28] DA	Extrapolation Gauss Ampere and Exponential	06	6,90	14,52
		07		14,68
		07		14,79
Boukli [28] DM	Extrapolation Gauss Ampere and Exponential	06	6,93	14,52
		07		14,68
		07		14,79
Guemmadi [29]	Extrapolation Gauss Ampere	04	6,39	
		08		
		07		
		07		
Mehamdia [31]	Extrapolation Exponential	06	6,91	14,74

To this end, the following procedure discusses the stages of how to perform laboratory tests in a new experimental program.

As a first point, it is necessary to carry out laboratory tests on a wide range of concretes including all practically possible variations. This because - as clearly described for the examined concretes above - partial curves cannot capture the real shape and consequently do not provide much information about the {\text{R}}_{\text{C}28} variation curves.

The next point is to perform experimental tests on concretes using a precise value of ({\text{G}\text{F}\text{l}\text{M}}_{\text{g}}) and ({\text{F}\text{D}}_{\text{g}}) and by varying the type and dosage of the components in order to establish how the different curves unfold for the same ({\text{G}\text{F}\text{l}\text{M}}_{\text{g}}) value and thereby control the influence of two (type and dosage) parameters of the concretes components.

The last point - to complete the procedure - is to work with a new value of ({\text{G}\text{F}\text{l}\text{M}}_{\text{g}}) and to vary the other design-mix ingredients as previously stated, in order to highlight in a special way the influence of both ({\text{G}\text{F}\text{l}\text{M}}_{\text{g}}) and

({\text{F}\text{D}}_{\text{g}}). The expressions used - Gauss-Ampere function - for instance, suggest that the only difference will be attributed to the difference between the values of ({\text{G}\text{F}\text{l}\text{M}}_{\text{g}}):

{\text{R}}_{\text{C}28}={\text{Y}}_{\text{o}}+\text{A}\times {\text{e}}^{{-(0.5\times (\text{X}-
{\text{X}}_{\text{o}\text{p}\text{t}\text{i}\text{m}\text{a}\text{l}}))}^{2}/{{\omega }}^{2}} (Eq. 18)

This fact may not be true since we are working with different basic granular mixes for which the porosity value may be different but the volume of the paste is still the same and therefore different concretes are obtained. However, this change is required to understand whether there is correlation when the ({\text{G}\text{F}\text{l}\text{M}}_{\text{g}}) and ({\text{F}\text{D}}_{\text{g}}) values are considered as variables or otherwise to find out how dependent are the variables {(\text{Y}}_{0}), (\text{A}) and (\text{w}) according to the value of ({\text{G}\text{F}\text{l}\text{M}}_{\text{g}}). In particular, although the optimal value of ({\text{G}\text{F}\text{l}\text{M}}_{\text{g}}) was similar for all the works on dry granular mixes of [9], this may not necessarily true for concretes using granular mixes incorporated with cement, fines, mineral additions and water.

- First statement

In the mixtures used by [29], the total dosage (cement and fines: C + F) is equal to 350 kg/m^3 for the majority of concretes, with the exception of those represented by the curve (18% (C + F) for which {\text{S}}_{\text{c}\text{f}}=729.72 {\text{m}}^{2}/\text{k}\text{g}). In this case, the four concretes contain dosages (C + F) vary from 250 to 450 kg/m^3, while the fine dosage is always equal to 18% of the total dosage (C + F).

- Second statement

One of the complicating problems observed and that caused difficulties in obtaining results for the prediction of ({\text{R}}_{\text{C}28}) is attributed to the limited range of concretes prepared by each author. To clearly address the urgent need for concretes to be investigated in more exhaustive manner, we took the curve of [29] with fines whose specific surface is equal to 729,72 m^2/kg. This curve is based on a collection of data for tests performed on eight (points) different concretes, as illustrated in Fig. 13(b_2). This figure shows the fit of the curves obtained with a reduced data of the eight concrete types tested. If, for instance, the number of points is limited to 3 or 4 concretes, the fit may only be made with the simplified exponential function. Interestingly, as the points number increases and larger interval sweeps are considered, fitting results provided using this Gauss-Ampere function are closer to the real curve.

- Third statement

In every type of the concretes explored, fittings based on Gauss-Ampère law provide the determination of ({\text{R}}_{\text{C}28}) maximum value along with optimum value for the dosage of cement, fines and mineral additions. However, this process can only be applied for separate basic granular mixture categories analysis, see ({\text{G}\text{F}\text{l}\text{M}}_{\text{g}}) value in (Eq. 9).

As a quick and possibly expedient problem, we take the example represented by Fig. 13(a_2) of the work of [29]. These are concretes with ({\text{G}\text{F}\text{l}\text{M}}_{\text{g}}=\text{6,38}), ({\text{F}\text{D}}_{\text{g}}=\text{2,56}) and ({\text{S}}_{\text{S}}= 206,53 m^2/kg) for the fine included using different rates (0 to 42%). The fittings shown in Fig. 6 (b) enables to determine the maximum ({\text{R}}_{\text{C}28}) and the optimal dosage of cement, fine and mineral additions for a constant volume of water, knowing the value of ({\text{G}\text{F}\text{l}\text{M}}_{\text{g}}), see (Eq. 9). We therefore find that:

{\text{R}}_{\text{C}28\text{m}\text{a}\text{x}} = 43,34 MPa

And

\left(\text{C}\times {\text{K}}_{\text{C}}\times {\text{S}}_{\text{S}\text{c}}\right)
+

\left({\text{M}}_{\text{f}}\times {\text{S}}_{\text{S}\text{f}}\right)
+
(\sum _{\text{i}}{\text{M}\text{i}}_{\text{A}\text{d}\text{m}}\times {\text{K}\text{i}}_{\text{A}\text{d}\text{m}}\times
{\text{S}\text{i}}_{\text{S}\text{A}\text{d}\text{m}})
/(1000\times \text{W})=\text{1,36}
This last expression reduces to

(\text{C}\times {\text{K}}_{\text{C}}\times {\text{S}}_{\text{S}\text{c}})
+
{(\text{M}}_{\text{f}}\times {\text{S}}_{\text{S}\text{f}})
/(1000\times \text{W})=\text{1,36}
in the case of no mineral addition.

Several theoretical solutions are suited for evaluating the cement-fine couple. As part of this discussion, we mention only three combinations, for instance. Hence, the first combination corresponds to (\text{C}=\text{606,50} \text{k}\text{g}/{\text{m}}^{3}) and ({\text{M}}_{\text{f}}=0 \text{k}\text{g}/{\text{m}}^{3}). The second one is for (\text{C}=\text{592,45} \text{k}\text{g}/{\text{m}}^{3}) and (5% of cement + fine), i.e. ({\text{M}}_{\text{f}}=\text{31,16} \text{k}\text{g}/{\text{m}}^{3}) and finally, the last combination comprises 18% of cement + fine) and therefore (\text{C}=\text{552,01} \text{k}\text{g}/{\text{m}}^{3}) and ({\text{M}}_{\text{f}}=\text{121,16} \text{k}\text{g}/{\text{m}}^{3}). Of course, these propositions remain only theoretical solutions because the total mass and volume of cement and fines vary in each case.

In the cases examined, we have, respectively, three (\text{189,53} \text{l}/{\text{m}}^{3}, \text{197,07} \text{l}/{\text{m}}^{3} and \text{218,90} \text{l}/{\text{m}}^{3}) water dosages with a constant water dosage equal to 198 \text{l}/{\text{m}}^{3}. The question that remains to be raised is what is the adequate volume of aggregate to be used, since the total volume of the ingredients together with that of air, is equal to 1000 litres. However, the volume or masse of the aggregate may be determined in each case - if necessary - by keeping the same value of the (GFIM). However, we have to specify that - by reducing the quantity of aggregate - we strongly reduce the porosity. This indicates that it is a different concrete compared to the concretes produced previously with the same mass of aggregate.

As an alternative solution, we may also proceed by reducing the quantity of the water incorporated but it is likely not to know whether the corresponding point still remain on the same curve. Indeed, the suggested three theoretical solutions involve operating with high rates of cement dosage. These may not be suitable in practice. In addition, they effectively generate some extra troubles because of cost, shrinkage and creep. Again, the remaining question is to what extent these theoretical solutions adequately reflect the concretes physico-chemical phenomena, even though Fig. 13(a_2) shows a decrease in ({\text{R}}_{\text{C}28}) for a value of "(\text{C}\times {\text{K}}_{\text{C}}\times {\text{S}}_{\text{S}\text{c}})(+(\text{M}}_{\text{f}}\times {\text{S}}_{\text{S}\text{f}}\left)\right)/(1000\times \text{W})" greater than 1.36.

- Fourth statement

It should be noted that the same Gauss-Ampere function was used to identify the evolution of the compactness of basic granular mixtures (see section 3.2). We must add, however, that for concrete the introduction of the paste can disturb the arrangement of the grains when the related volume is greater than the volume of the pores. This indicates the link between the fractal model and the two-phase model of concrete with the excess paste theory. Use of the simplified exponential formula tend to no longer affect the ({\text{R}}_{\text{C}28}) value, starting from a certain dosage level of solid grains (cement, fines and mineral additions). This effectively is contrasted with the known related phenomena. In addition, the reached ({\text{R}}_{\text{C}28}) value increases significantly and appears not to well relate to experimental observations.

- Fifth statement

It seems clear - in the light of the above experimental results - that for a known basic granular mixture with fixed ({\text{G}\text{F}\text{l}\text{M}}_{\text{g}}) i.e. for a given porosity, the volume variation of paste may lead to different concretes. This is why practitioners and researchers use the Standard Test of NF EN 206 [40] to determine the true class of cement but always using the same standardized basic granular mixture. Also, it should be noted that assessment of optimal workability of concretes is an additional difficulty with regard to the choice of the paste dosage and type. Therefore, there is recognition of the need of further investigations in order to remove the difficulties.

7. Conclusion

This work explicitly aimed to present a new paradigm for the study and control of the mechanical compressive strength of concrete. The use of the two-phase model and the fractal granular identification modulus enable to evaluate the influence of a set of parameters related to the incorporated ingredients, namely the cement (dosage, type and specific surface), the fines (dosage and specific surface), mineral additions (dosage, activity coefficient and specific surface) and of course water on ({\text{R}}_{\text{C}28}).

We started with the same basic granular mixture, no cement, no fines and no addition of minerals to end up with different concretes with - of course - the addition of these latter components and water. Although the concrete samples studied were prepared by different authors as well as at different dates and with different methods and arrangements, this did not prevent the proposed approach from yielding this new paradigm, as illustrated by (Eq. 13).

In addition to the necessity of having another work to follow this work, as we mentioned at the beginning, the purpose should be the time interval for the contrast of concrete to be very wide. However, similar results currently obtained by extending the same model to concrete with additives prove the exploratory value of this approach. It will also be necessary to extend these results to other types of concrete such as self-uniforming concrete and high-performance concrete.

The accuracy of the results obtained even indicates that concrete is far from being this material undergoing a complex study because it calls into question what seemed to be the dispersions inherent in all experimental work.

It is recalled that the model was applied to grains of aggregates whose real shape was not spherical (random angular shape). Also, the approach was limited to the use of the standardized class of cement due to lack of to have been able to use the true class and that in spite of the obvious error relating to each determination of ({\text{R}}_{\text{C}28}), see (Eq. 13).

The use of the two-phase model of concrete coupled with the fractal model of granular distribution allows us to clarify and better understand the theory of excess paste which has been proposed in various works.

The didactic aspect of this approach is an asset because we quickly understand how to produce concrete with maximum mechanical resistance. However, it remains to verify the adequacy of the various curves obtained with the real physico-chemical phenomena.

Of course, we are still far from claiming to offer one or more ideal and general grain size curves since we can only compare concretes made with the same basic granular mixture. It remains for us to study how to access the case where the basic granular mixture is different in order to apply it to the wide range of concretes used.

The question of the optimal value of FD remains and seems more complex than that advanced in the work of [9]; for dry granular mixtures. Indeed, it is necessary to take into account the influence of the addition of other components (theory of excess paste) as well as the workability property and the associated impact on the values of the other concrete ingredients.

Declarations

- **Funding**: (This research did not receive any specific grant from funding agencies in the public, commercial, or not-for-profit sectors.)
- **Competing interests:** The authors declare that they have no competing interests
- **Availability of data and material:** The datasets generated during and/or analysed during the current study are available from the corresponding author on reasonable request.
- **Code availability:** (The software OriginPro2016 N° EFBAFCE9D61338D0 version 9.70.188)
- **Authors' contributions**

The authors contribute to the study of a new model, which contributes to the design of concrete. The main task of this research work is accomplished within the framework of a doctorate thesis, in addition to the supervision and support role in the scientific research, as this research involves a close collaboration between the authors.

- **Acknowledgements**

The authors would like to thank Professor Rabah SOLTANI of the Laboratoire de Mécanique des Structures & Stabilité des Constructions (LM2SC), Civil Engineering Department, University of Sciences and Technology Mohamed BOUDIAF, BP 1505 El Menaouar, 31000 Oran (Algeria), for his comprehensive efforts in revising and editing the manuscript.

References

1. Féret, R. Sur la compacité des mortiers hydrauliques. Annales des Ponts et Chaussées. Édition. Paris. Vve. C. Dunod. Série 1892;**7**(4): 5-164.
2. Duff A. Abrams, Design of Concrete Mixtures. Bulletin No 1, Structural Materials Research Laboratory Lewis Institute, Chicago, 1918; [Consulted le 2016].
3. Bolomey J. Granulation et prévision de la résistance probable des bétons. Bulletin technique de la Suisse romande 1936;**7**(62): 73-78. https://www.e-periodica.ch/cntmng?pid=bts-002:1936:62:95
4. De Larrard F. Structures granulaires et formulation des bétons. France: LCPC Nantes; 2000.
5. Chidiac, S.E. Moutassem, F. Mahmoodzadeh, F. Compressive strength model for concrete. Mag. Concr. Res 2013;**65**(9): 557–572. Doi.org/10.1680/macr.12.00167.
6. Koutas LN, Tetta Z, Dionysios A, Bournas C, Thanasis PE, Triantafillou M. Strengthening of Concrete Structures with Textile Reinforced Mortars: State-of-the-Art Review, J. Compos. Constr 2019;**23**(1): 03118001. Doi.org/10.1061/(ASCE)0899-1561(2008)20:7(459).
7. Boukli, HMA, Ghomari F, Khelidj A. Probabilistic Modelling of Compressive Strength of Concrete Using Response Surface Methodology and Neural Networks. Arab J Sci Eng 2014;**39** (6):4451-4460. Doi.org/10.1007/s13369-014-1139-y.
8. Caquot A. Le rôle des matériaux inertes dans le béton. Mémoire de la Société des Ingénieurs Civils de France 1937;**76** (5) 562-582.
9. Chouicha K. La dimension fractale et l'étendue granulaire comme paramètres d'identification des mélanges granulaires, Mater Struct 2006;39:665–681. Doi.org/10.1617/s11527-006-9113-0.
10. Sebsadji SK, Chouicha K. Determining periodic representative volumes of concrete mixtures based on the fractal analysis, Int J Sold Struct 2012;**49** 2941–2950. Doi.org/10.1016/j.ijsolstr.2012.05.017.
11. Powers TC. The Nature of Concrete. American Society for Testing and Materials STP No, 1966, 169-A, 61-72. Skokie, Illinois.
12. Yang CC, Huang R. A two-phase model for predicting the compressive strength of concrete. Cement and Concrete Research 1996;**26**(10): 1567-1577. https://doi.org/10.1016/0008-8846(96)00137-8.
13. Klemczak B, Batog M, Pilch M. Assessment of concrete strength development models with regard to concretes with low clinker cements. Arch Civ Mech Eng 2006;**16** 235-247. Doi.org/10.1016/j.acme.2015.10.008.
14. ACI. 211.1-91, American, Concrete Institute, Standard Practice for Selecting Proportions for Normal, Heavyweight, and Mass Concrete, Farmington Hills Michigan; 2002.
15. Benkemoun N, Rachel G, Roubin E, Colliat JB. Poroelastic two-phase material modeling: theoretical formulation and embedded finite element method implementation. International Journal for Numerical and Analytical Methods in Geomechanics 2015;**39**(12): 1255-1275. https://doi.org/10.1002/nag.2351.
16. Bonifaz E, Baus J, Lantsoght E. Modeling Concrete Material Structure: A Two-Phase Meso Finite Element Model. Journal of Multiscale Modelling 2017;**08**(02): 1750004. Doi:10.1142/S1756973717500044.
17. Rouibi M, Chouicha K. Porosity assessment of granular mixtures intended for concrete using the fractal model of particle-size distribution.Construction and Building Materials 2021;**293**: 123492. Doi.org/10.1016/j.conbuildmat.2021.123492.
18. Turcotte DL. Fractales et chaos en géologie et géophysique. University Press, Cambridge, 1997, ISBN-13 978 0521567336. Doi.org/10.1017/CBO9781139174695.

19. Lecomte A, Thomas A. Caractère fractal des mélanges granulaires pour bétons de haute compacité. Mater Struct 1992 ;**25**(5):255–264. Doi.org/10.1007/BF02472666.
20. Dhir RK, McCarthy MJ, Paine KA. Engineering property and structural design relationships for new and developing concretes. Mater Struct 2005;**38**(1):1-9. Doi.org/10.1007/BF02480568.
21. De Larrard F, Lecomte A, Mechling JM. Résistance à la compression de bétons hydrauliques au squelette granulaire non optimisé. Bulletin LCPC 2001 ;**234** 4378: 89-105. https://www.ifsttar.fr/collections/BLPCpdfs/blpc_234_86-106.pdf.
22. Zennir A. Bétons calcaires en Lorraine : utilisation des granulats du bajocien de Viterne (54) pour la formulation de bétons courants. Corpus, University of Nancy France 1996. ID: 193383996
23. Meddah MS, Zitouni S, Belâabes S. Effect of content and particle size distribution of coarse aggregate on the compressive strength of concrete.Constr Build Mater 2010;24:505–512. Doi:10.1016/j.conbuildmat.2009.10.009.
24. Hager-Gawęska I, Tracz T, Śliwiński J, Krzemień K, Hang HI. The influence of aggregate type on the physical and mechanical properties of high-performance concrete subjected to high temperature. PhD Thesis, Ecole Nationale des Ponts et Chaussées et Ecole Polytechnique de Cracovie : Fire Mater John Wiley & Sons, Ltd 2015. DOI: 10.1002/fam.2318.
25. Roziere E, Loukili A, El Hachem R, Grondin F. Durability of concrete exposed to leaching and external sulphate attacks. Cem Concr Res 2009;**39**(12):1188-1198.Doi.org/10.1016/j.cemconres.2009.07.021.
26. Quiroga PN, Fowler DW. The effects of aggregates characteristics on the performance of Portland cement concrete, Report ICAR 104-1F, Project Number 104, University of Texas at 2003Austin, http://hdl.handle.net/2152/35333.
27. Achour T, Lecomte A, Ben Ouezdou M, Mensi R, Judi BI. Contribution of the fillers limestones to the paste-aggregate bond. Tunisian examples. Mater Struct 2008;**41**: 815–830. Doi:10.1617/s11527-007-9287-0.
28. Boukli HMA, F Ghomari, Khelidj A. Compressive Strengths of Concrete Formulated with Algerian Local Materials, Jordan J Civ Eng 2009;3 (2).
29. Guemmadi Z, Resheidat M, Chabil H, Toumi B. Modeling the Influence of Limestone Filler on Concrete: A Novel Approach for Strength and Cost. Jordan J Civ Eng 2009;**3**(2):158-171.
30. Judi BI, Lecomte A, Ben-Ouezdou M, Achour T. Use of limestone sands and fillers in concrete without superplasticizer, Cem Concr Compos 2012;**34**(6): 771-780.Doi.org/10.1016/j.cemconcomp.2012.02.010.
31. Mehamdia A, Benouis A. Contribution à l'estimation de la perméabilité a l'air des betons par les vitesses des ultrasons University of Bayonne France 2015. https://hal.archives-ouvertes.fr/hal-01167663.
32. Rabehi M, Mezghiche B, Guettala S. Correlation between initial absorption of the cover concrete, the compressive strength and carbonation depth, Constr Build Mater 2013;**45**:123–129.Doi.org/10.1016/j.conbuildmat.2013.03.074
33. Benouis A, Grini A. Effect of Concrete Mixtures on Estimation of Porosity by Ultrasonic Velocity. Nondestructive Test Mater Str 2011;**6**: 309-316 Doi 1007/978-94-007-0723-8_44.
34. Saadani S, Comportement des bétons à base de granulats recycles, Thesis University of Constantine Algeria 2000.
35. Mennaai A, Contribution à l'étude rhéologique d'un béton à hautes performances (BHP) local, , Thesis, University Skikda Algeria 2008.
36. Boutiba A, Chaid R, Laurent ML, Jauberthie R. Effect of sulfur aggregates on mechanical resistance and durability for SFRHPC with the addition of slag. MATEC Web of Conferences 2014;11 03005 CC BY 4.0. (2014). Doi.org/10.1051/matecconf/20141103005.
37. Chopra P, Sharma RK, Kumar M. Prediction of Compressive Strength of Concrete Using Artificial Neural Network and Genetic Programming. Hindawi Advances in Civ Eng 2018. Doi.org/10.1155/2018/5481705.
38. Moutassem F, Chidiac SE. Assessment of Concrete Compressive Strength Prediction Models. KSCE. J Civ. Eng 2016 ;**20**(1): 343-358. Doi.org/10.1007/s12205-015-0722-4.
39. Yang S, Lim Y. Mechanical strength and drying shrinkage properties of RCA concretes produced from old railway concrete sleepers using by a modified EMV method. Constr Build Mater 2018;**185**(10): 499-507, Doi.org/10.1016/j.conbuildmat.2018.07.074 762.
40. AFNOR NF EN 206 + A1, Classification index Concrete - Specification, Performance, Production and Conformity 2016; P 18-325, ICS: 91.080.40; 91,100.30 AFNOR Paris.

Figures

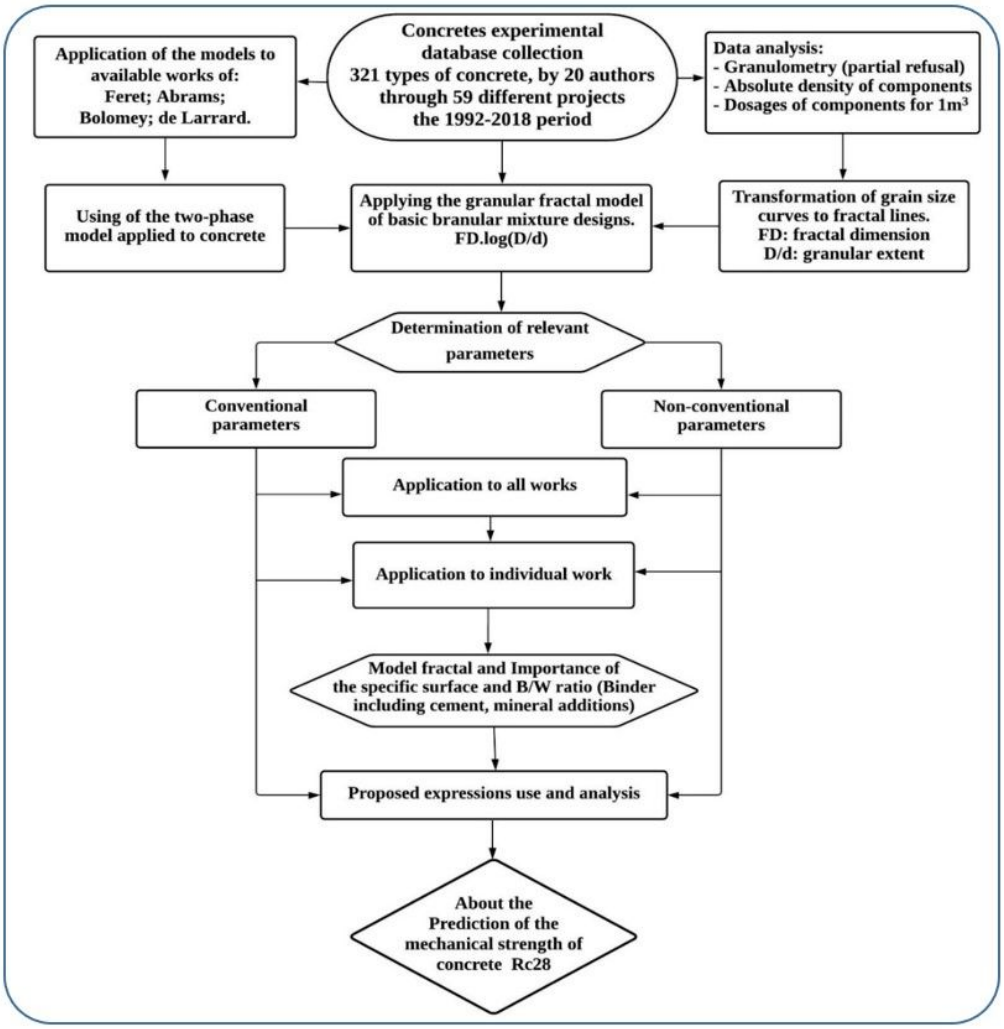

Figure 1

Design Automation diagram for our new model, based on collected data

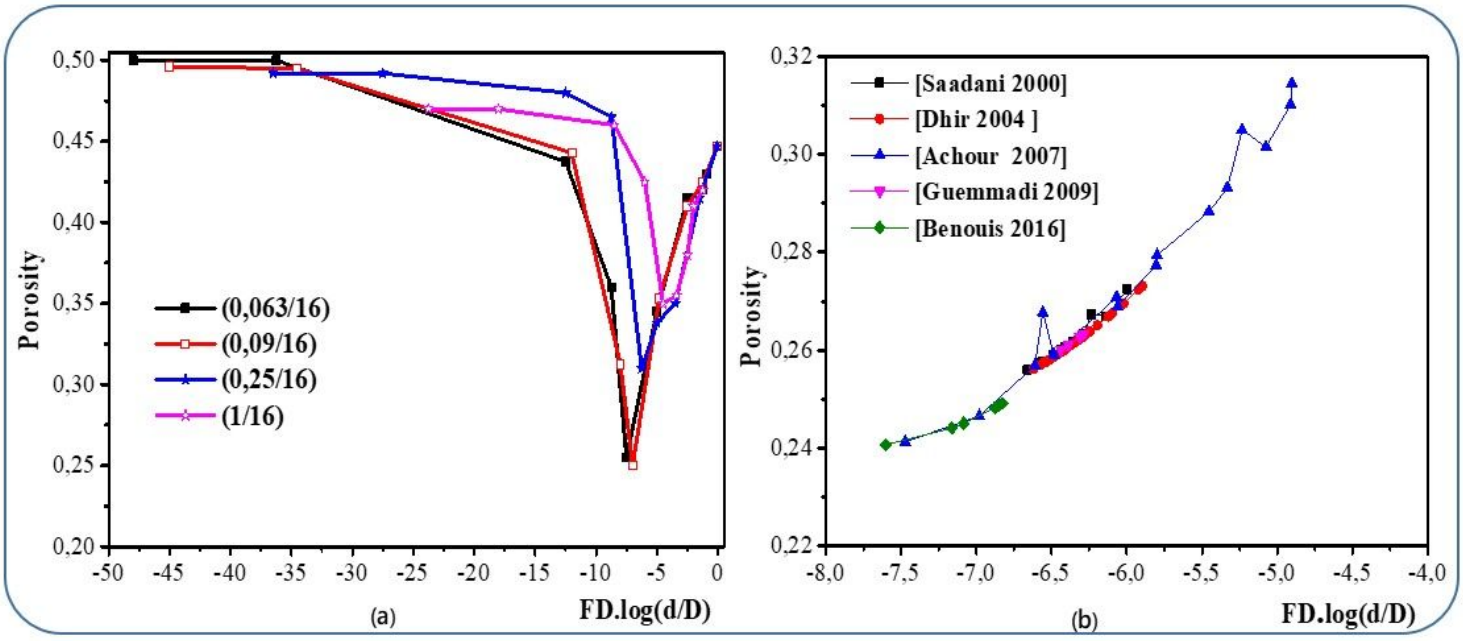

Figure 2

Evolution of porosity in terms of fractal model: (a) Porosity model of [9]; and (b) Application on some mix designs

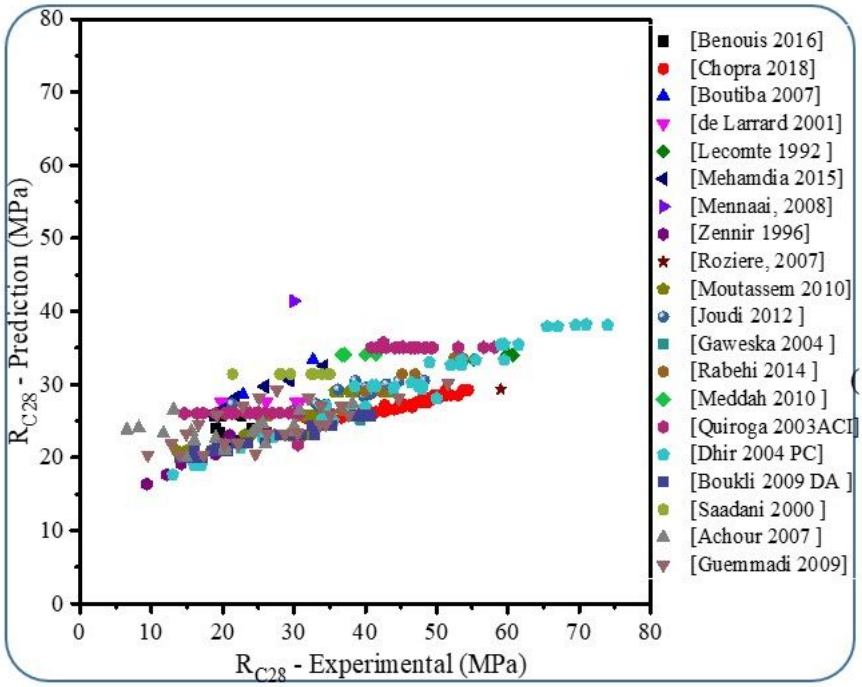

Figure 3

Comparisons of experimental results with available models.

Application of the formula of Feret [1]

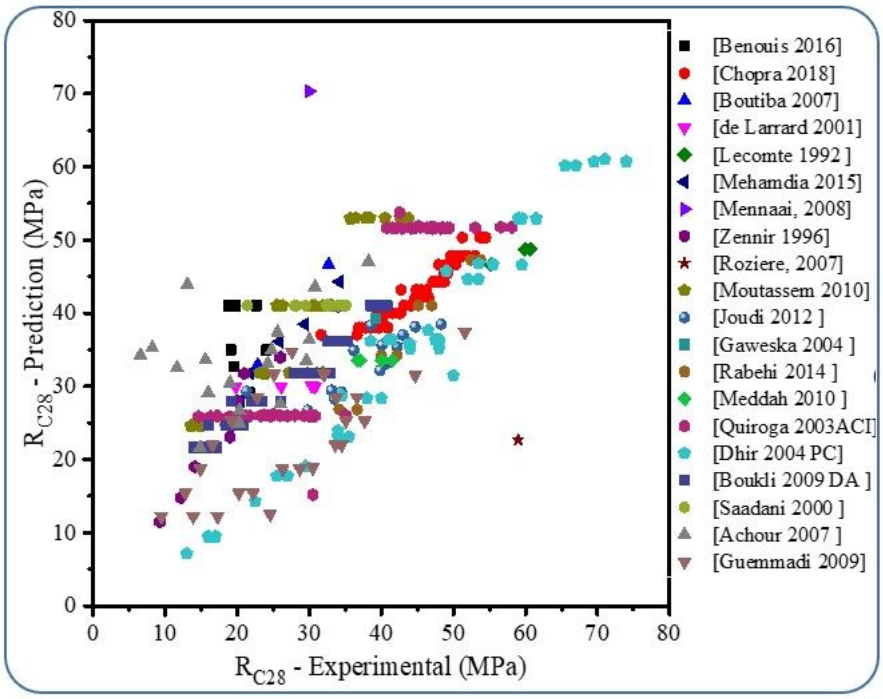

Figure 4

Comparisons of experimental results with available models.

Application of the formula of Abrams [2]

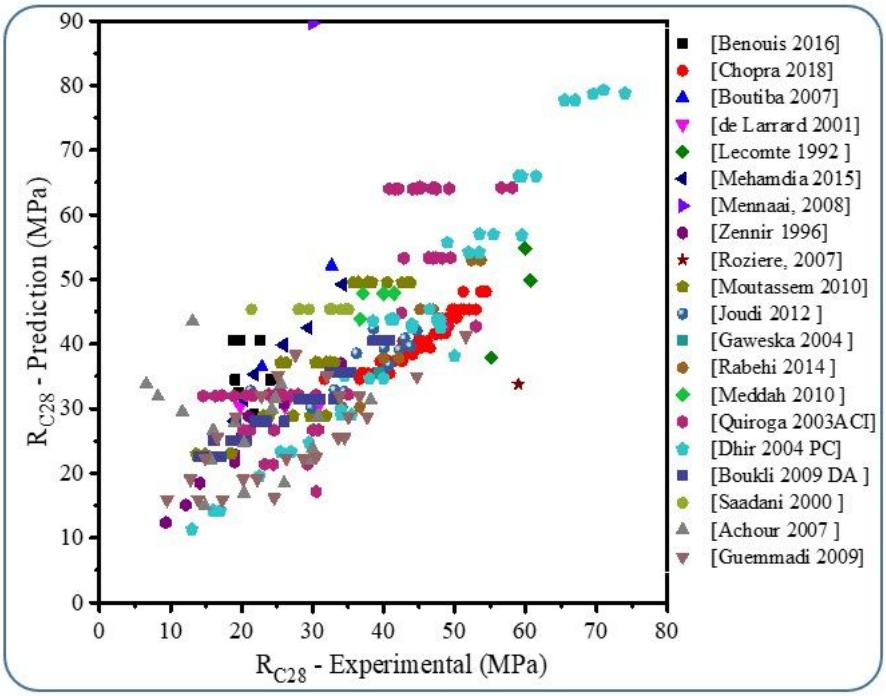

Figure 5

Comparisons of experimental results with available models.

Application of the formula of Bolomey [3]

Figure 6

Comparisons of experimental results with available models.

Application of the formula of De Larrard [4]

Figure 7

Examples of grains size curves transformed into fractal straight lines the work of [20]:

(a) Particle size curves and (b) Associated converted fractal lines

Figure 8

Effect of (c/w) ratio on R_{C28}

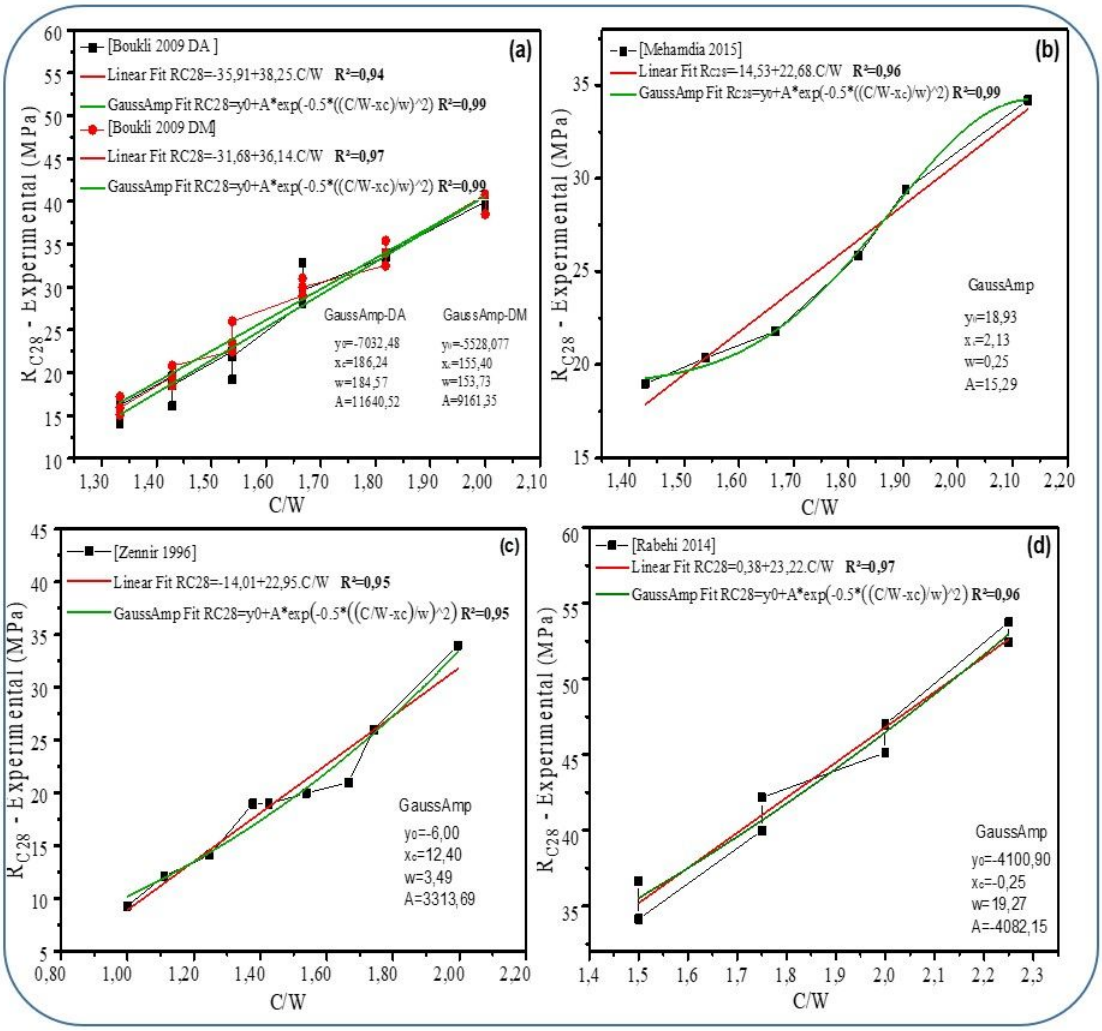

Figure 9

R_{C28} - C/W evolution of some authors' concretes with increased correlations (a), (b), (c), (d)

Figure 10

R_{C28} - C/W evolution of some authors' concretes with low to reasonable correlations (a), (b), (c), (d)

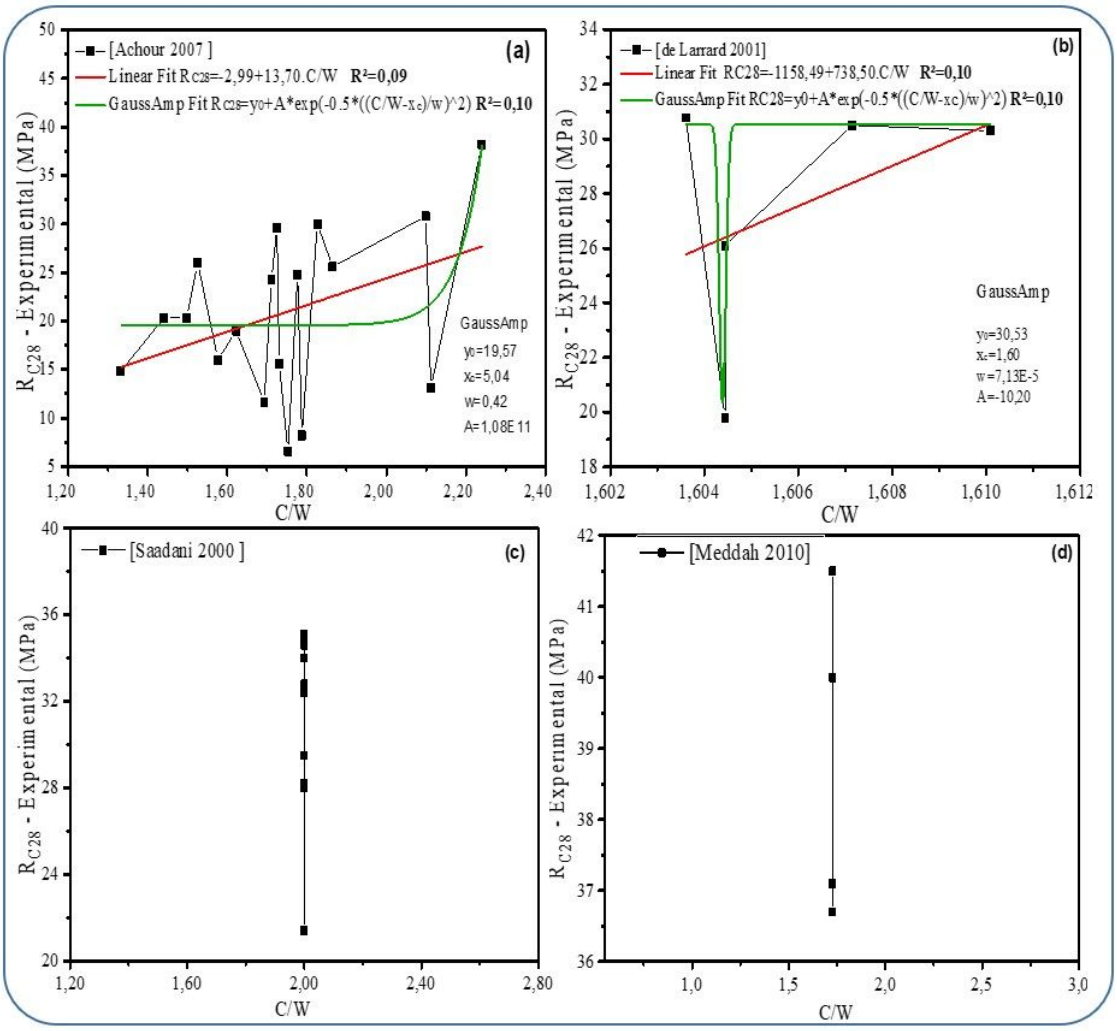

Figure 11

R_{C28} - C/W evolution of some authors' concretes with zero correlations (a), (b), (c), (d)

Figure 12

Influence of Por(D/d) of cement free granular mixes [9]; on compressive strength R_{C28}

Figure 13

Experimental curves illustrating strength R_{C28} in terms of C/W: (a) Complete curve - R_{C28} - C/W [29]; (b) R_{C28} - C/W in terms of FD_g, $GFIM_g$ & fines S_{Sf} [29], (c) Complete curve R_{C28} - C/W [32]; (d) R_{C28} - C/W in terms of cement S_{Sc} [32].

Figure 14

Experimental curves and fitting of concrete types: (a), (b) Gross experimental curves using values of all concretes and of $GFIM_g$ & $GFIM_c$ [28], (c), (d) Gross experimental curves using values of all concretes of $GFIM_g$ and S_{sc} [29], (e), (f) Gross experimental curve using values of $GFIM_g$ [22, 31];

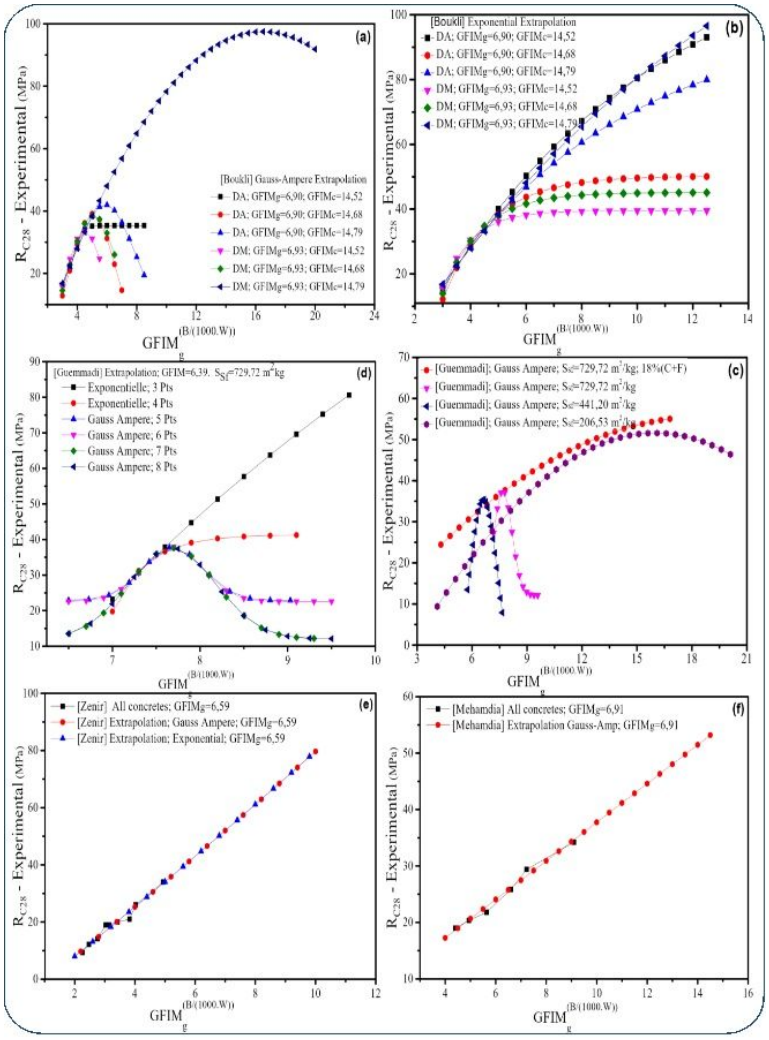

Figure 15

Experimental curves and fitting of concrete types: (a, b, c) Fitting according to the Gauss Ampere/Exponential function using values of $GFIM_g/GFIM_c/S_{Sf}$ [28, 29], (d) Shapes of curves obtained using fitting in terms of number of points (concretes) [29], (e, f) Fitting according to the Gauss Ampere/Exponential function using values of $GFIM_g$ [22, 31];

Supplementary Files

This is a list of supplementary files associated with this preprint. Click to download.

- SupplementaryMaterials.docx